Int J Adv Manuf Technol (2015) 78:1813–1826
DOI 10.1007/s00170-014-6770-y

ORIGINAL ARTICLE

Multi-objective optimization design of injection molding process parameters based on the improved efficient global optimization algorithm and non-dominated sorting-based genetic algorithm

Jian Zhao · Gengdong Cheng · Shilun Ruan · Zheng Li

Received: 22 August 2014 / Accepted: 29 December 2014 / Published online: 18 January 2015

Abstract This paper develops a framework that tackles the Pareto optimum of injection process parameters for multi-objective optimization of the quality of plastic part. The processing parameters such as injection time, melt temperature, packing time, packing pressure, cooling temperature, and cooling time are studied as model variables. The quality of plastic part is measured by warp, volumetric shrinkage, and sink marks, which is to be minimized. The two-stage optimization system is proposed in this study. In the first stage, an improved efficient global optimization (IEGO) algorithm is adopted to approximate the nonlinear relationship between processing parameters and the measures of the part quality. In the second stage, non-dominated sorting-based genetic algorithm II (NSGA-II) is used to find a much better spread of design solutions and better convergence near the true Pareto optimal front. A cover of liquid crystal display part is optimized to show the method. The results show that the Pareto fronts obtained by NSGA-II are distributed uniformly, and this algorithm has good convergence and robustness. The pair-wise Pareto frontiers show that there is a significant trade-off between warpage and volumetric shrinkage, and there is no significant trade-off between sink marks and volumetric shrinkage and between sink marks and warpage.

Keywords Injection molding · Kriging surrogate model · IEGO · Multi-objective optimization design · NSGA-II

J. Zhao (✉) · G. Cheng · S. Ruan · Z. Li
State Key Laboratory of Structural Analysis for Industrial Equipment, Department of Engineering Mechanics, Dalian University of Technology, Dalian 116024, China
e-mail: zhaojian3028@mail.dlut.edu.cn

1 Introduction

Plastic injection molding is an important manufacturing technique to plastic products due to the advantages of high production efficiency, competitive cost, light weight, and good flexibility to complex geometry. The cycle of plastic injection molding consists of six stages: clamping, filling, packing, cooling, opening, and ejecting. The quality of plastic injection molding parts depends on the materials, part and mold designs, and the process parameters required to manufacture them. Defects in the products, such as warp, shrinkage, sink marks, and residual stress, are caused by many factors during the production process. Therefore, numerous studies have been conducted on the optimization design of plastic injection molding process parameters. For instance, Dang [1] reviewed the state-of-the-art of the process parameter optimization for plastic injection molding and proposed two general frameworks for simulation-based optimization of injection molding process parameter, including direct optimization and metamodeling optimization. Wang et al. [2] improved the compressive property of the valve body by the application of computer-aided engineering integrating with the Taguchi method. However, Taguchi method can only find the best specified process parameter level combination which includes the discrete setting values of process parameters. Farshi et al. [3] minimized the warpage and shrinkage defects of plastic parts by sequential simplex method. Applying artificial neural networks (ANN) has been proposed to improve conventional Taguchi parameter design and is capable of effectively treating continuous parameter values. Wang et al. [4] developed an ANN model to understand the relationship between plastic injection molding process parameters and shrinkage, and the test results on the performance of the ANN model showed that it could predict the shrinkage with reasonable accuracy.

In order to yield a product with high precision, designers often need to consider the quality of plastic parts which

involve many product properties that may be incommensurate and competing. Thus, quality can be viewed as an attempt to satisfy many objectives. The designers will have to make tradeoffs amongst the properties so that all of them are satisfied simultaneously and the process operates at the best point. However, for many multi-objective optimization design problems, the researchers usually make the multi-objective problems into single-objective optimization problems and apply ANN and evolutionary algorithms to attain the final optimal process parameters. Yin et al. [5] established a multi-objective optimization to optimize the process parameters during plastic injection molding on the basis of the finite element simulation software Moldflow, Orthogonal experiment method, BP neural network, as well as genetic algorithm. A series of combination of weights of optimization objectives were specified to the multi-objective optimization model. Mehat and Kamaruddin [6] developed a new constitutive approach in solving multi-response problems using a combination of single responses through the Taguchi method. For example, the combination response for the single responses A an B can be obtained as follows: $S/N_{AB}=S/N_A+S/N_B$. The S/N ratio is quoted in dB units and can be defined as follows: $S/N=-10Log_{10}(MSD)$, where MSD is the mean square deviation for the responses being studied. Deng et al. [7] developed a multi-objective GA optimization strategy, where the objective functions may be defined by the designers, including using different criteria and/or weights. Huang and Tang [8] presented the technique for order preference by similarity to ideal solution which gives a performance measure on the qualities to be optimized in order to resolve multiple qualities problems. The experimental layout in the Taguchi method provided training samples of a neural network. The genetic algorithm was aimed at finding parameter values in a continuous solution space to optimize a performance measure on denier and tenacity qualities based on the neural network. Hsu et al. [9] presented an integrated approach using neural networks, exponential desirability functions, and genetic algorithms to optimize parameter design problems with multiple responses. In optimization procedure, the trade-off solutions obtained by using the predefined strategy would be sensitive to the weight factors chosen in converting the multi-objective to a single-objective function. In order to solve the complex multi-objective optimal performance design of large-scale injection molding machines, Wei et al. [10] studied non-dominated sorting genetic algorithm II (NSGA-II) to find a much better spread of design solutions and better convergence near the true Pareto optimal front. Wei et al. [11] discussed rough set-based support vector clustering method to improve the computational efficiency of Strength Pareto Evolutionary Algorithm (SPEA).

Table 1 Properties of ABS AF303 material

Properties of the material	
Commercial product name	ABS AF303
Solid density (g/cm^3)	1.0541
Melt density (g/cm^3)	0.96622
Moldflow viscosity index	VI(240)0089
Recommended mold temperature (°C)	60
Recommended meld temperature (°C)	200
Material characteristics	Amorphous
Ejection temperature (°C)	85
Modulus of elasticity (MPa)	2240
Poisson ratio	0.392
Shear modulus (MPa)	804.6
Thermal conductivity W/m-C	0.16 at 200 °C

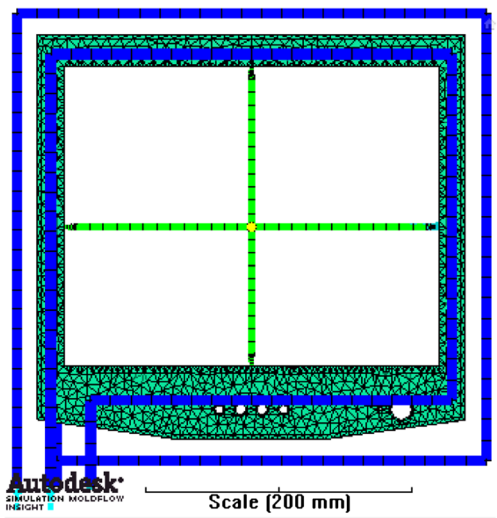

Fig. 1 The finite element model of a cover of liquid crystal display part with cooling channels and runner system

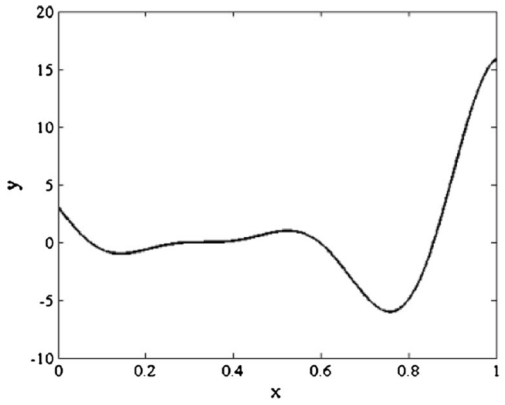

Fig. 2 One variable test function

The number of external stocks was reduced, and the optimal Pareto solution was determined by eliminating the uncertainty in the artificial priority election. The multi-objective optimization of the HT1600X1N injection molding machine was taken as an example. Ferreira et al. [12, 13] developed a framework that tackled the design of an injection molding system in a global way, through structural, thermal, rheological, and mechanical domain integration. A building approach by modules was adopted for process integration, where all different analysis codes were connected through an integration software in order to automate the iterative procedure of the optimization process.

All the researches cited beforehand accomplished optimization of plastic injection molding process parameters and mainly focused on the procedure of optimization. However, a clear and reliable prediction model that could be used as the surrogate model during process optimization is still required. Plastic part defects are nonlinear, implicit function of the process parameters. So far, several models have been used for fitness approximation. The most popular ones are polynomials, the Kriging surrogate model, the feedforward neural networks, and support vector machines. One advantage of using Kriging models is that a confidence interval of the estimation can be obtained without much additional computational cost. In this study, the Kriging surrogate model is adopted to approximate the nonlinear relationship between processing parameters and the optimization objectives, replacing the expensive finite element analysis of optimization objectives. Warp, volumetric shrinkage, and sink marks are challenging defects in injection molding and investigated as the optimization objectives. Injection time, melt temperature, packing time, packing pressure, cooling temperature, and cooling time are considered to be the design variables. Surrogate-based optimization strategies use both the prediction and the uncertainty estimates offered by surrogates to select the next sample point for an expensive simulation. The efficient global optimization (EGO) al-

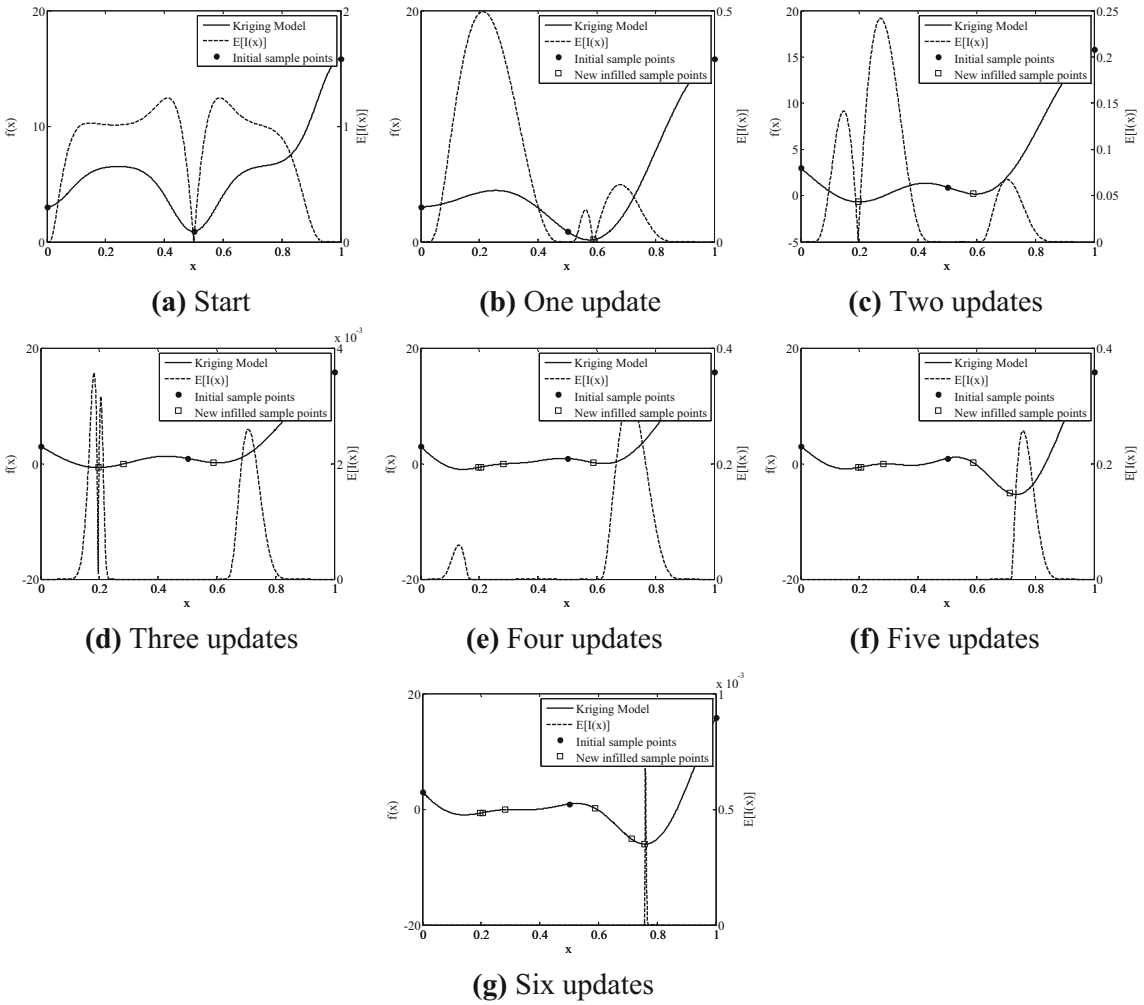

Fig. 3 **a**–**g** The progress of a search of the one variable test function applying EGO

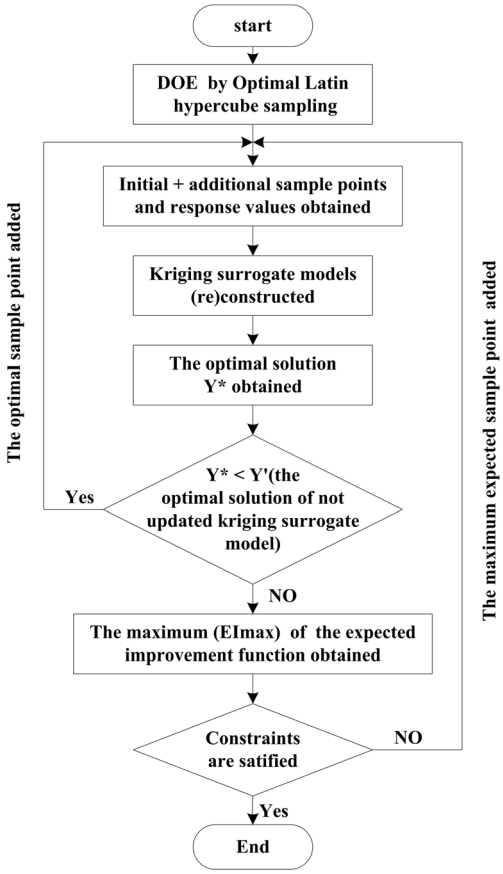

Fig. 4 IEGO algorithm flowchart

gorithm selects the next point to be sampled by maximizing the expected improvement. However, EGO algorithm may present premature convergence and influence the solution accuracy. In this paper, the improved efficient global optimization algorithm is proposed. The optimization iterations are based on the improved efficient global optimization (IEGO) algorithm in the first stage, and in the second stage, NSGA-II algorithm is used to find a much better spread of design solutions and better convergence near the true Pareto optimal front.

2 Front shell of the LCD TV

As shown in Fig. 1 is the finite element model of the front shell of LCD TV. Finite element analyses of the thin shell part utilized in this study are performed using commercial software Moldflow. The length, width, and thickness of the front shell are 320, 305, and 3.2 mm, respectively. The geometry of this plastic part is discretized using Fusion mesh by Moldflow, which is a commercial software based on hybrid finite element/finite difference method for solving pressure, flow, and temperature fields. The analysis model consists of 9886 elements. The front surface must have a very high appearance quality to meet the esthetic requirements. Therefore, any surface defects, such as flow mark, sink mark, warp and volume shrinkage, etc., should be completely avoided. The plastic material used for the front shell is ABS AF303, supplied by LG chemical. Table 1 gives the properties of the plastic material in detail.

3 Description of optimization methodology

The optimization methodology including the improved efficient global optimization methodology based on the Kriging surrogate model for developing the proposed approach is briefly introduced below.

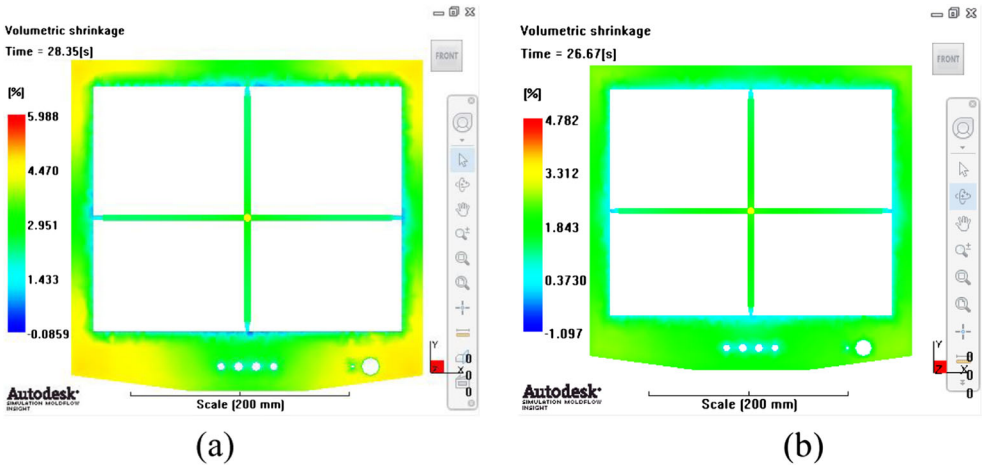

Fig. 5 **a** The volumetric shrinkage distribution before and **b** after optimization process

Table 2 The optimum design of volumetric shrinkage before and after optimization process

Parameters	t_i	T_{Me}	P_P	P_t	C_T	C_t	Volumetric shrinkage (%)
The optimum design of the initial sample design	0.734	185	81.25	8.62	32.19	19	5.988
The optimum design after applying IEGO	0.507	185.96	151.4	9.998	24.596	16.165	4.782
Related rate (%)	30.93	0.52	86.34	15.99	23.59	14.92	20.14

3.1 Kriging surrogate model

Kriging model was initially developed by geologists to estimate the properties of sampled minerals over an area of interest given a set of sampled sites; it was also introduced at about the same time in the field of spatial statistics as a probabilistic model to predict values over a finite space. The Kriging model is described as a way of modeling the function as a realization of a stochastic process; thus, it is named a stochastic process model. The mathematical form of a Kriging model has two parts as shown in Eq. 1. The first part is a known polynomial function often taken as constant. The second part $z(x)$ is the correlation function which represents a stochastic process with mean at 0, variance σ^2, and nonzero covariance as shown in Eq. 2.

$$y(x) = \sum_{j=1}^{P} \beta_j f_j(x) + z(x) = f(x)^T \beta + z(x) \tag{1}$$

$$\begin{cases} E[z(x)] = 0 \\ \mathrm{Var}[z(x)] = \sigma^2 \\ \mathrm{cov}\left[z\left(x^i\right) z\left(x^j\right)\right] = \sigma^2 R\left(\theta; x^i, x^j\right) \end{cases} \tag{2}$$

where $R(\theta;x^i,x^j)$ is the correlation function between any two of the sample points, in which $x^i=[x_1^i,x_2^i,\cdots x_m^i]$ is the ith sample point with m variables, and all correlation function values of the sample points compose the correlation matrix R. The correlation function controls the smoothness of the resulting Kriging model, the influence of other nearby points, and the differentiability of the surface by quantifying the correlation between the observations [14]. There are many potential functions that can be used to quantify the correlation between the observations. The correlation function used in this work is shown in Eq. 3 and defined with only one parameter, θ, which controls the range of influence of nearby points.

$$R\left(\theta; x^i, x^j\right) = \prod_{l}^{m} \exp\left(-\theta_l \left(x_l^i - x_l^j\right)^2\right) \tag{3}$$

We adopt the maximum likelihood approach to estimate Kriging parameters β, θ as is implemented in the DACE toolbox by Lophaven et al. [15].

3.2 Efficient global optimization methodology

The EGO algorithm begins by fitting a DACE model to a set of initial points specified by "space-filling" experimental design. After evaluating the function on the initial design, the parameters of a DACE model are fit using maximum likelihood estimation. Once the initial DACE surface is fit, optimization process is conducted iteratively. First, the expected improvement is maximized using optimization algorithm. If the expected improvement is less than 0.1 % of the best current function value, the iterative process is terminated. Otherwise, the new sample point is selected where expected

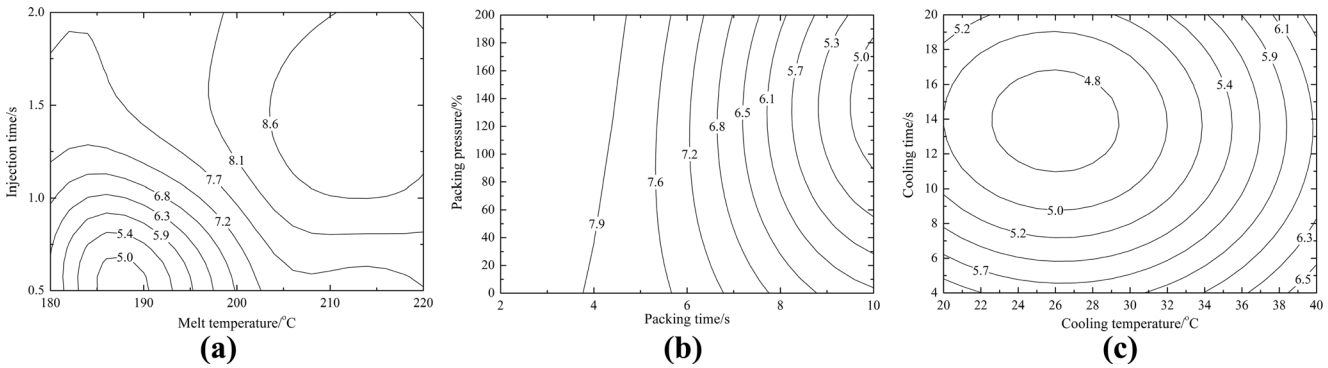

Fig. 6 **a**–**c** Contours for the effect of the processing parameters on the volumetric shrinkage of the part

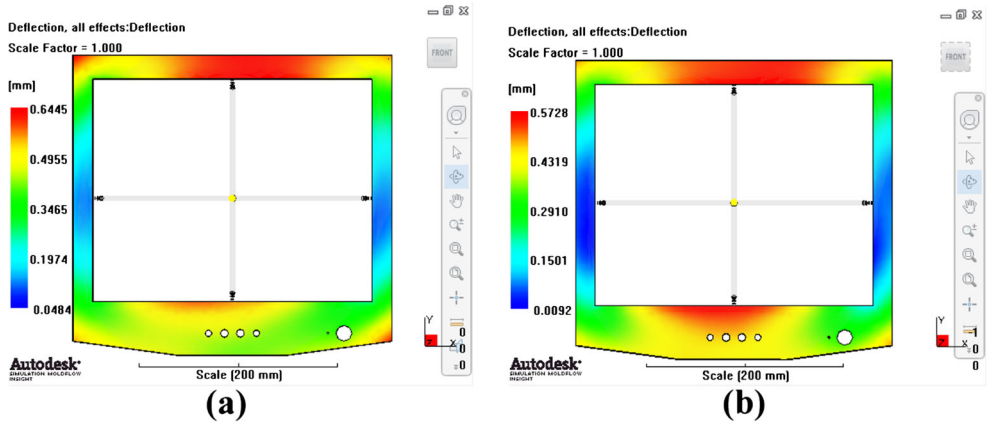

Fig. 7 **a** The warp distribution before and **b** after optimization process

improvement is maximized, re-estimate the DACE parameters with maximum likelihood, and iterate. The expected improvement criterion is computed as follows:

$$E(I) = \left[Y_{\min} - \hat{Y}(x)\right]\Phi\left(\frac{Y_{\min} - \hat{Y}(x)}{\sigma(x)}\right) + \sigma(x)\phi\left(\frac{Y_{\min} - \hat{Y}(x)}{\sigma(x)}\right) \quad (4)$$

where $\Phi(.)$ and $\phi(.)$ are the cumulative density function and probability density function of a normal distribution, respectively, $Y_{\min}$ is the present best sample, $\hat{Y}(x)$ is the Kriging prediction, and $\sigma(x)$ is the prediction standard deviation [16].

The details of one variable test function are given as Eq. 5, and Fig. 2 is its plot. Figure 3 shows the progress of a maximum $E[I(x)]$-based optimization of the one variable test function. We selected three initial sample points to construct Kriging surrogate model of the example problem. The situation is shown after six updates. The solid line of plots shows the Kriging prediction of the function based on the sample data, whereas the dotted line shows the expected improvement in the prediction. After six updates, the minimum $f_{\min} = -6.0204$ of the function was found. Although the search of one variable cannot be considered as a credible optimization problem, the progress of the search is indicative of that of many higher dimensional problems.

$$f(x) = (6x-2)^2 \sin(12x-4) \quad x \in [0, 1] \quad f_{\min} = -6.0207 \quad (5)$$

3.3 The improved efficient global optimization methodology

One of the major difficulties in applying optimization in many engineering problems is that each function evaluation requires a complete simulation which is computationally expensive, so optimization algorithm efficiency is very important for designers. The above EGO algorithm is efficient in many cases, but it may present premature convergence and influence the solution accuracy. In this paper, the improved efficient global

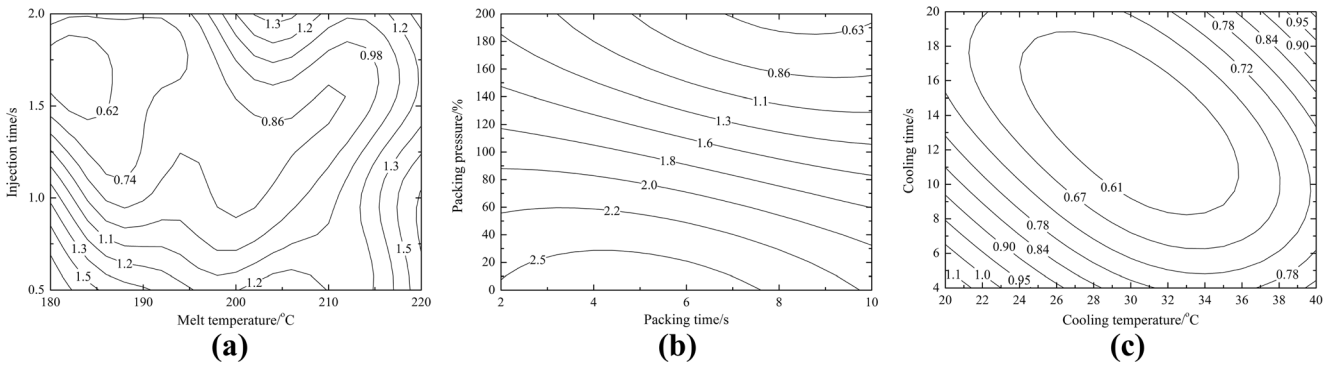

Fig. 8 **a**–**c** Contours for the effect of the processing parameters on the warp of the part

Table 3 The optimum design of warp before and after optimization process

Parameters	t_i	T_{Me}	P_P	P_t	C_T	C_t	Warp (mm)
The optimum design of the initial sample design	1.836	191.25	200	7.5	24.06	12.504	0.6445
The optimum design after applying IEGO	1.591	180.69	199	7.834	27.01	16.155	0.5728
Related rate (%)	13.34	5.52	0.5	4.45	12.26	29.20	11.13

optimization algorithm is proposed. The first improvement is the infill criteria. In each iteration of reconstruction of Kriging model, the optimal design of the recently constructed Kriging model is added to sample points and update Kriging model if it is better than the previous optimum. Otherwise, the design which maximizes the expected improvement function is added to sample points. In other words, the optimal design of each iteration is preferentially considered in the global search. The second improvement is that the more strict convergence conditions are implemented as follows:

$$|x_k - x_{k-1}| \le \varepsilon_1 \tag{6}$$

$$|f_{\min}(x_k) - f_{\min}(x_{k-1})| \le \varepsilon_2 \tag{7}$$

$$\frac{|f_{\min}(x_k) - f_{\min}(x_{k-1})|}{f_{\min}(x_k)} \le \varepsilon_3 \tag{8}$$

where x_k and x_{k-1} are optimal designs of Kriging models during the (k-1)th iteration and kth iteration, respectively, $f_{\min}(x_k)$ and $f_{\min}(x_{k-1})$ are optimal solutions at x_k and x_{k-1}. The convergence condition (Eq. 6) is used in this study which conquers premature convergence. Figure 4 presents the flowchart of the IEGO. The IEGO is schematically described below:

(1) Optimal Latin hypercube sampling technique is used to generate the initial sample points. Initial sample points of $m=10n$ have been suggested, where m is the initial sample size and n is the number of variables.
(2) Construct the Kriging-based model from initial sample points.
(3) Find optimum design of the Kriging model.
(4) If optimal solution is less than the optimal solution of not updated Kriging model, add optimal design to sample points and update Kriging model. Go to step (3).
(5) Find the design that maximizes the expected improvement function.
(6) If the expected improvement is less than tolerance (TOL), stop. The suggested value for TOL is 0.1 %.
(7) Sample the function where expected improvement is maximized and update Kriging. Go to step (3).

4 Reduction of the part defects by optimizing process parameters applying IEGO

In the first optimization procedure, three objective functions are considered, namely warp minimization, volumetric shrinkage minimization, and sink marks minimization. The minimum design problem can be stated as follows:

$$\begin{aligned} &\text{find}: \; x = [t_i,\ T_{Me},\ P_P,\ P_t,\ C_T,\ C_t] \\ &\text{Minimize}: \; \text{Warp}(x);\ \text{Volumetric shrinkage}(x);\ \text{Sink marks}(x) \\ &s.t.: \; 0.5s \le t_i \le 2s \\ &\qquad 180^\circ C \le T_{Me} \le 220^\circ C \\ &\qquad 0 \le P_P \le 200\% \\ &\qquad 2s \le P_t \le 10s \\ &\qquad 20^\circ C \le C_T \le 40^\circ C \\ &\qquad 4s \le C_t \le 20s \end{aligned} \tag{9}$$

where x are the variables, representing process parameters. The processing parameters involved in experimental design are injection time, melt temperature, packing pressure, packing time, cooling temperature, and cooling time, which were represented by the t_i, T_{Me}, P_P, P_t, C_T, and C_t, respectively. The ranges of cooling temperature and melt temperature are based on the recommended values in Moldflow Plastics Insight, and the ranges of in injection time, packing pressure, packing time, and cooling time are determined by the experience of the manufacturer. Warp(x), Volumetric shrinkage(x), and Sink marks(x) are quantified warp

Table 4 The optimum design of sink marks before optimization process

Parameters	t_i	T_{Me}	P_P	P_t	C_T	C_t	Sink marks (%)
The optimum design of the initial sample design	1.836	191.25	200	7.5	24.06	12.5	0

Table 5 The optimum design of sink marks in the optimization process

Parameters	t_i	T_{Me}	P_P	P_t	C_T	C_t	Sink marks (%)
The optimum designs in the optimization process	1.757	183.74	192.2	7.584	28.696	9.899	0
	1.526	190.64	197.7	7.008	31.026	8.156	
	1.473	181.19	199.4	5.685	32.27	9.402	
	1.258	184.48	198.7	8.752	34.8	7.43	
	1.36	183.61	195	5.81	30.857	11.15	
	1.191	186.94	199.5	7.865	25.117	7.594	
	1.553	184.14	193	6.417	34.313	12.35	
	1.738	193.35	200	7.228	25.224	13.054	
	1.732	187.04	197.8	8.183	23.677	8.515	
	1.394	185.11	194.8	8.59	30.948	7.666	
	1.171	181.7	200	6.7	28.12	12.569	
	1.863	189.43	200	7.904	25.87	11.133	
	1.403	196.35	198.4	7.303	31.082	13.044	
	1.586	180.5	187.5	6.767	37.002	8.197	
	1.526	182.7	188.6	6.457	34.403	9.627	
	1.118	181.61	198.1	8.121	30.821	17.831	
	1.487	191.53	196.8	7.277	28.342	17.686	
	1.227	186.46	199.5	7.626	29.943	16.027	
	1.378	180.67	189.5	9.019	37.074	18.763	
	1.325	184.85	198.5	7.757	23.476	15.288	
	1.510	180.88	189.3	6.755	34.09	18.065	
	1.478	184.03	196.1	7.493	23.734	9.709	
	1.334	188.65	197.5	6.771	23.606	12.245	
	1.654	188.88	197.4	6.104	21.982	13.502	
	1.685	193.76	200	9.795	39.529	19.78	
	1.464	188.35	199.4	8.586	37.949	12.97	
	1.866	189.21	199.6	6.501	23.323	10.963	
	1.953	193.83	198.3	9.367	39.955	19.79	
	1.513	191.18	196.8	7.602	27.612	13.585	
	1.468	180.79	199.4	8.941	37.293	11.541	
Related rate (%)	74.73	8.78	6.67	72.3	81.76	166.34	

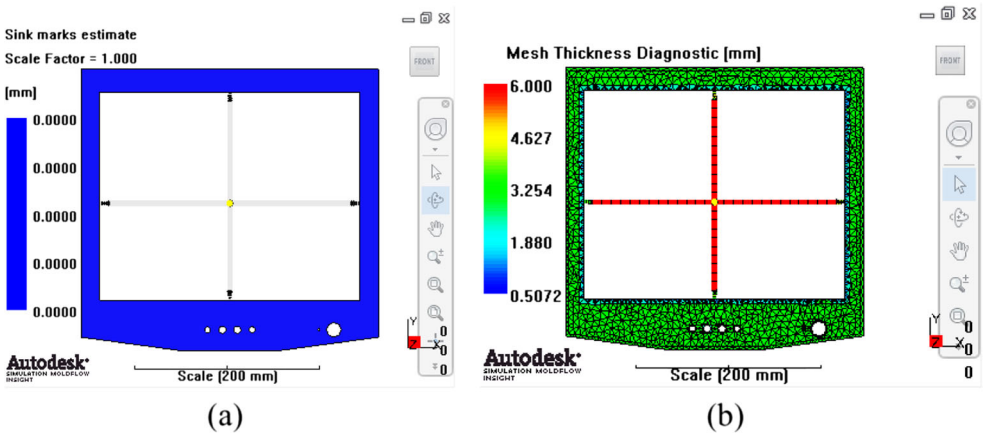

Fig. 9 **a** The sink marks distribution of the optimum design and **b** thickness distribution of the part

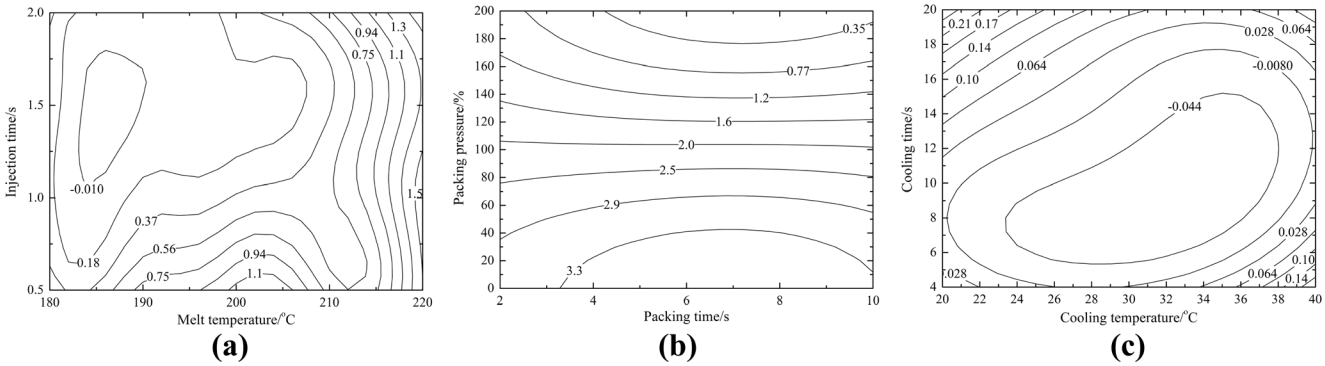

Fig. 10 **a**–**c** Contours for the effect of the processing parameters on the sink marks of the part

value, volumetric shrinkage value, and sink marks value, respectively, which will be replaced by an approximate function based on the Kriging surrogate model in optimization iterations.

The optimization procedure of injection molding based on the IEGO algorithm is described as follows:

(1) Generate the initial sample points applying optimal Latin hypercube sampling approaches. In this work, a set of sample points with 65 points is obtained and run the Moldflow program to obtain the objective values for the initial sample points.
(2) Construct the Kriging surrogate model between each objective and the process parameters based on the trial sample points obtained.
(3) Optimized each objective based on the Kriging surrogate model applying IEGO algorithm until convergence criteria are satisfied.

Figure 5 shows the volumetric shrinkage distribution of the part before and after optimization. The location of maximum volumetric shrinkage of the molded part is the four corners before optimization process, and after optimization process, the distribution of volumetric shrinkage is uniform as shown in Fig. 5b. Table 2 gives injection molding parameters of maximum volumetric shrinkage before and after optimization. It is seen that maximum volumetric shrinkage is reduced by about 20.14 % after optimization. Figure 6 shows that the effect of the processing parameters on the volumetric shrinkage of the part under the condition where all other processing parameters are kept at their optimal value. The response surfaces based on contour diagrams as shown in Fig. 6 are both concave surfaces, which implies that the range of all processing parameters chosen in this experiment are appropriate and optimal volumetric shrinkage can be achieved and, therefore, the optimized set of process parameters can be determined.

The contour plot, as shown in Fig. 6a, reveals the volumetric shrinkage variation between the effect of melt temperature and injection time. According to the contour plot, it suggests that when the injection time is less than 1 s, the values of volumetric shrinkage for the melt temperature generally tend to first decrease slightly and then increase, and tend to increase to the

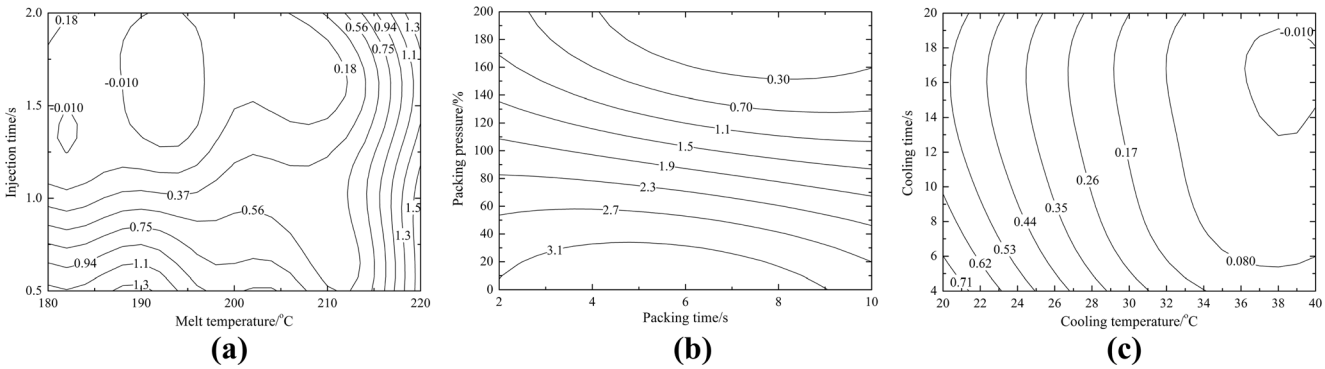

Fig. 11 **a**–**c** Contours for the effect of the processing parameters on the sink marks of the part

Table 6 Tuning parameters used in NSGA-II

Parameters	Values
Population size	500
Number of generations	100
Crossover probability	0.9
Crossover distribution index	10
Mutation distribution index	20

injection time from 1 to 2 s. In this study, an increase in melt temperature causes an increase in volumetric shrinkage because of the greater volume contraction. Too long of an injection time will lead to a decrease in the melt temperature and a non-uniform distribution of the end-of-fill temperature which will cause volumetric shrinkage. Figure 6b shows the volumetric shrinkage variation between the effect of packing time and packing pressure. As the packing time and packing pressure increase, the volumetric shrinkage decreases due to the fact that more material is injected into the cavity during packing stage. Comparing the three plots in Fig. 6, the cooling time and the cooling temperature also affect the volumetric shrinkage, but the effect on the volumetric shrinkage is much smaller based on the gradient of the volumetric shrinkage than that of other process parameters.

It is seen that maximum warp on the thin shell plastic model, which is 0.6445 mm before the optimization, is reduced to 0.5728 mm by about 11.13 % after optimization. The simulated warp is shown in Fig. 7. Warp is a distortion where the shape of the molded part deviates from the intended shape of the design. It is caused by volumetric shrinkage of the part in the cooling process, the residual flow and thermal stresses produced in the filling and packing process, and the non-uniform volume shrinkage of the part generated in the whole injection molding process. The comparison results show that the warp distributions before and after optimization process have the same tendency, as shown in Fig. 7. The maximum of the warp is located at the top and bottom gates where the imbalanced in-mold stresses are large.

Figure 8 shows that the effect of the processing parameters on the warp of the part. The warp variation between the effect of melt temperature and injection time is shown in Fig. 8a. A higher melt temperature can lead to a lower viscosity, which results in a lower cavity pressure and shear stress. However, as in literature reports [17, 18], during cooling stage, the higher the melt temperature, the higher the warp value. Short injection time will increase the cavity pressure and shear stress. On the contrary, long injection time will lead to a decrease in the melt temperature and a non-uniform distribution of the end-of-fill temperature. In this study, a long injection time and low melt temperature will decrease the warp. According to Fig. 8b, in can be noted that the warp decreases with the increase of packing pressure and packing time, and the packing pressure and the packing time are shown to have a significant effect on the volumetric shrinkage. Figure 8c shows that the influences of the cooling temperature and the cooling time are not so significant. A suitable cooling temperature and cooling time have a positive influence on warp reduction (Table 3).

From this study results, it can be concluded that sink marks is a multi-optimum function. Before optimization, the optimum design can be obtained from initial sample as shown in Table 4; however, the accuracy of the Kriging surrogate model is not satisfied with the convergence condition. Therefore, after 107 updates, the termination criterion is fulfilled. In the optimization process, there are 30 optimum designs to minimize sink marks within the optimal values of process parameters as shown in Table 5.

Sink marks is a depression or dimple on the part surface [19, 20]. It is caused by the relatively larger localized shrinkage of the plastic material. The larger localized shrinkage is resulted from the local thick-wall structure, such as ribs, bosses, etc. Generally, the more dramatic the thickness variation of the plastic part is, the larger the shrinkage difference is and consequently the more apparent the sink marks is. It can be clearly seen in Fig. 9b that the part thickness is uniform, and it is easy to obtain optimum process parameters of sink marks.

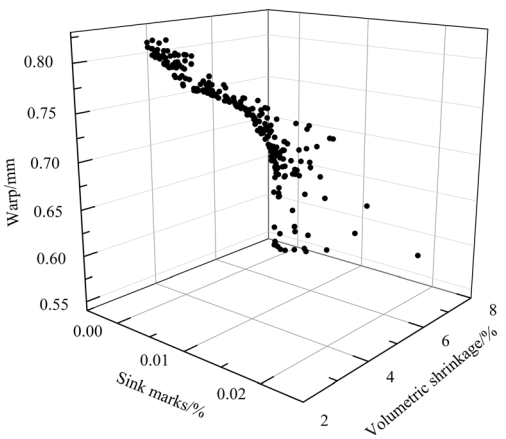

Fig. 12 Triple-objective Pareto frontier using the Kriging surrogate model updated by IEGO

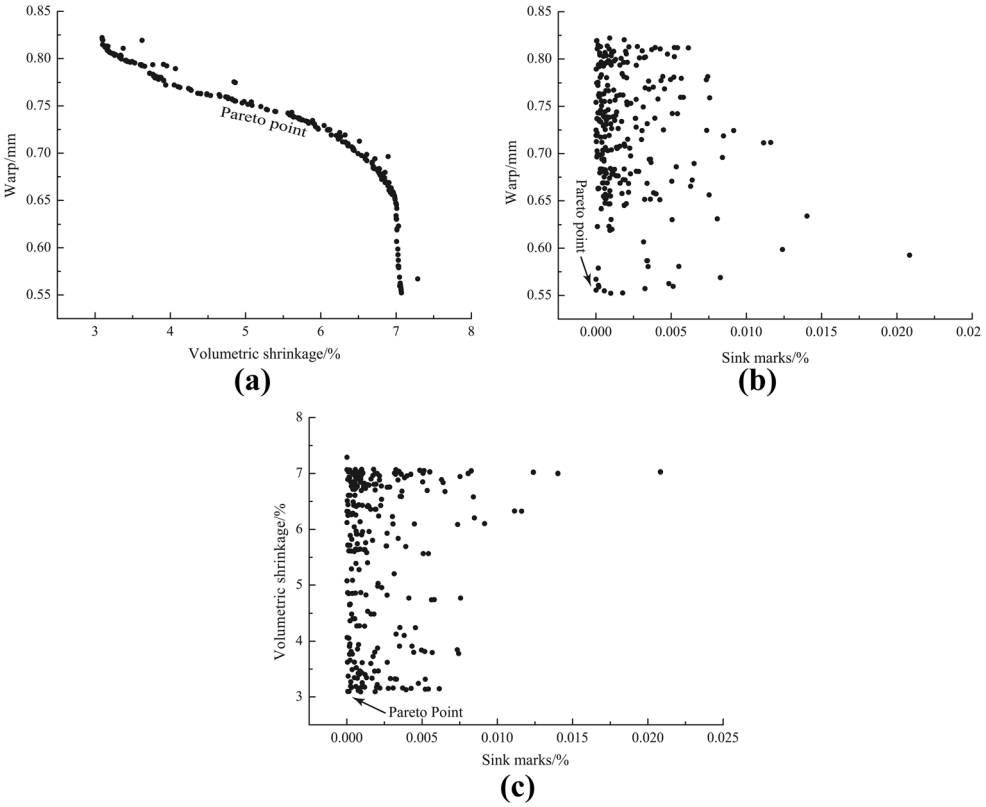

Fig. 13 **a**–**c** Pair-wise Pareto front using the Kriging surrogate model updated by IEGO

Figures 10 and 11 show that the effect of the processing parameters on the sink marks of the part under the condition where all other processing parameters are kept at their optimal value of the optimum design before the optimization process and of the last optimum design in the optimization process, respectively. Comparing the Figs. 10 and 11, the results reveal that the trend for contours under different condition is very similar. Low melt temperature will lead to decrease sink marks, but if melt temperature is too low, sink marks in thick section will be severe as a result. From Figs. 10a and 11a, it can be observed that a combination of decreased melt temperature with increased injection time will lead to rapidly reduce in sink marks. Increasing the packing pressure and packing time can decrease the sink marks as shown in Figs. 10b and 11b. In Fig. 10c, the value of the sink marks will decrease first and increase subsequently while increasing the value of cooling tem-

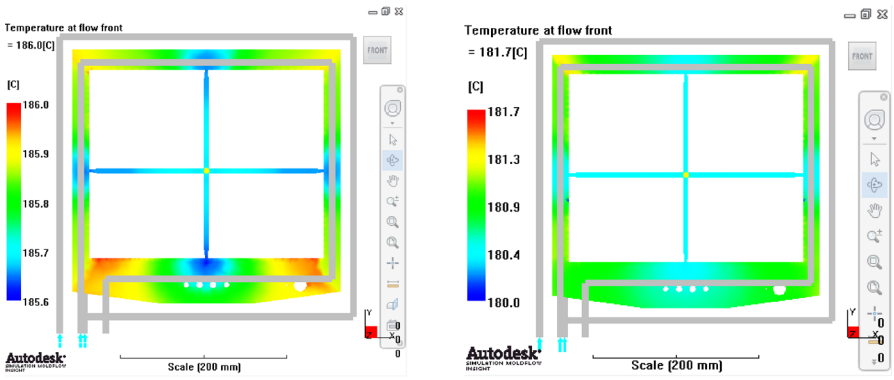

Fig. 14 **a**, **b** The temperature at flow front of the different design

(a) the optimum design of the volumetric shrinkage (b) the optimum design of the warp

Table 7 The optimum design of Pareto point between volumetric shrinkage and sink marks

Parameters	t_i	T_{Me}	P_P	P_t	C_T	C_t	Volumetric shrinkage (%)	Sink marks (%)
The optimum design of the Pareto point	0.5193	183.5888	199.769	9.761	21.7994	16.5697	4.418	0.0365

perature and cooling time; the center area of the ellipse is the best sink marks of the part. Increasing the value of cooling temperature in combination with increased cooling time will cause a reduction in sink marks as shown in Fig. 11c. From Figs.10c and 11c, cooling temperature and cooling time variation have minor influence on the sink marks.

5 Proposed multi-objective optimization approach

In order to globally optimize the plastic part quality as a system, the warp, volumetric shrinkage, and sink marks should be optimized as objective functions simultaneously. To undertake this optimization, a multi-objective genetic algorithm (MOGA) is adopted. MOGA optimization is carried out using the NSGA-II in iSIGHT-FD 5.0. Fast and Elitism NSGA-II is a suitable method that can satisfy the goals of multi-objective optimization [20]. NSGA-II uses elitism principle and crowded comparison operator that ranks the population based on both Pareto dominance and region density. This crowded comparison makes the NSGA-II considerably faster and convergent and also provides the ability to find a diverse set of solutions in comparison with the other methods [21]. Operational parameters used in NSGA-II are listed in Table 6.

The triple-objective Pareto frontier is shown in Fig. 12, and the pair-wise Pareto frontiers after IEGO algorithm are presented as in Fig. 13. The results show that the Pareto fronts obtained by NSGA-II are distributed uniformly, and this algorithm has good convergence and robustness.

The pair-wise Pareto frontiers in Fig. 13a show that there is a significant trade-off between warpage and volumetric shrinkage. As volumetric shrinkage is increased to 7 %, warpage can be reduced to below 0.55 mm. Comparing Figs. 6a and 8a, an apparent trend is observed that injection time is the significant factor affecting volumetric shrinkage and warp differently. In Table 2, injection time of optimum design of volumetric shrinkage before and after applying IEGO are 0.734 and 0.507, respectively, and injection time of optimum design of warp before and after applying IEGO are 1.836 and 1.591 in Table 3, respectively. The comparison of the results shows that the shorter injection time, the more uniform the temperature distribution is as shown in Fig. 14. When the temperature distribution uniformity is increased, the volumetric shrinkage is decreased. For a long injection time, material can be introduced into the cavity under lower injection pressure, which will contribute to decrease residual stress and molecular orientation. This can lead to reduce the warp. Therefore, with the increase of the injection time, the value of the warp is reduced as shown in Fig. 8a. It can be found that there is not a design point to make the volumetric shrinkage and warp functions to be optimal simultaneously. Therefore, the designer can select one point in practice from the Pareto optimal solutions shown in Fig. 13a according to the different requirements on product quality.

The pair-wise Pareto frontiers in Fig. 13 show that there is no significant trade-off between sink marks and volumetric shrinkage and between sink marks and warpage. As described above, sink marks increase with the thickness increasing, but in this study, the main plane of the part is thin and the thickness distribution is uniform; therefore, sink marks of the part can be decreased easily. From Figs. 8 and 10, the results reveal that the trend for contours for warp and for sink marks at different process parameters is very similar. The minimum area of volumetric shrinkage and the minimum area of sink marks partly intersect as shown in Figs. 6 and 10. Therefore, in Fig. 13, there is one design point to make the sink marks and warp to be optimal simultaneously, and one design point to make the sink marks and volumetric shrinkage to be optimal simultaneously. And Tables 7 and 8 show the two Pareto optimal solutions, which further validate the effectiveness of the proposed method.

Table 8 The optimum design of Pareto point between warp and sink marks

Parameters	t_i	T_{Me}	P_P	P_t	C_T	C_t	Warp (mm)	Sink marks (%)
The optimum design of the Pareto point	1.591	180.69	199	7.834	27.01	16.155	0.5728	0

6 Conclusions

The main objective of this study is to develop a framework that tackles the multi-objective optimization design of a plastic injection molding system in a global way. A two-stage approach is employed based on the IEGO and non-dominated sorting-based genetic algorithm II (NSGA-II). Firstly, the IEGO algorithm is proposed. In traditional EGO algorithm, expected improvement function is introduced to identify the new sample point by considering the prediction and mean squared error of Kriging surrogate model during the optimization procedure. Premature convergence may exit when the range of the objective function is too large in EGO algorithm. In this paper, the optimal solution of the Kriging surrogate model is preferentially considered, and the convergence conditions are increased to overcome premature convergence in IEGO algorithm. The modified algorithm is applied to a plastic injection optimization problem. Initial sampling designs are obtained using optimal Latin hypercube method, and the Kriging surrogate model is adopted to approximate the nonlinear relationship between processing parameters and the maximum warp, maximum volumetric shrinkage, and maximum sink marks of the part. Processing parameters such as injection time, melt temperature, packing time, packing pressure, cooling temperature, and cooling time are studied. The IEGO algorithm is proposed to modify the Kriging surrogate model and improve the accuracy of the Kriging surrogate model.

In the second stage, the three accurate Kriging surrogate model are used to optimize multi-objective design. The presence of multiple objectives in a problem, in principle, gives rise to a set of optimal solutions (largely known as Pareto optimal solutions), instead of a single optimal solution. In the absence of any further information, one of these Pareto optimal solutions cannot be better than the other. NSGA-II performs well in multi-objective optimization which is able to find much better spread of solutions and better convergence near the true Pareto optimal front. NSGA-II algorithm is carried out in iSIGHT 5.0. The results show that the Pareto fronts obtained by NSGA-II are distributed uniformly, and this algorithm has good convergence and robustness. The pair-wise Pareto frontiers show that there is a significant trade-off between warpage and volumetric shrinkage, and there is no significant trade-off between sink marks and volumetric shrinkage and between sink marks and warpage.

Acknowledgments The authors gratefully acknowledge the financial support from the National Basic Research Program of China (No. 2012CB025905) and wish to thank Moldflow Corporation for making their simulation software available for this study.

References

1. Dang XP (2014) General frameworks for optimization of plastic injection molding process parameters. Simul Model Pract Theory 41(2):15–27
2. Wang YQ, Kim JG, Song JI (2014) Optimization of plastic injection molding process parameters for manufacturing a brake booster valve body. Mater Des 56(4):313–317
3. Farshi B, Gheshmi S, Miandoabchi E (2011) Optimization of injection molding process parameters using sequential simplex algorithm. Mater Des 32(1):414–423
4. Wang R, Zeng J, Feng X, Xia Y (2013) Evaluation of effect of plastic injection molding process parameters on shrinkage based on neural network simulation. J Macromol Sci B 52(1):206–221
5. Yin F, Mao H, Hua L (2011) A hybrid of back propagation neural network and genetic algorithm for optimization of injection molding process parameters. Mater Des 32(6):3457–3464
6. Mehat NM, Kamaruddin S (2011) Multi-response optimization of injection moulding processing parameters using the Taguchi method. Polym Plast Technol Eng 50(15):1519–1526
7. Deng YM, Lam YC, Britton GA (2004) Optimization of injection moulding conditions with user-definable objective functions based on a genetic algorithm. Int J Prod Res 42(7):1365–1390
8. Huang CC, Tang TT (2005) Parameter optimization in melt spinning by neural networks and genetic algorithms. Int J Adv Manuf Technol 27(11–12):1113–1118
9. Hsu CM, Su CT, Liao D (2003) A novel approach for optimizing the optical performance of the broadband tap coupler. Int J Syst Sci 34(3):215–226
10. Wei Z, Feng YX, Tan JR, Wang J-l, Z-k L (2008) Multi-objective performance optimal design of large-scale injection molding machine. Int J Adv Manuf Technol 41(3–4):242–249
11. Wei Z, Yang D, Wang X, Wang J (2009) Multi-objectives optimal model of heavy equipment using improved Strength Pareto Evolutionary Algorithm. Int J Adv Manuf Technol 45(3–4):389–396
12. Ferreira I, Weck O, Saraiva P, Cabral J (2009) Multidisciplinary optimization of injection molding systems. Struct Multidiscip Optim 41(4):621–635
13. Ferreira I, Cabral JA, Saraiva P, Oliveira MC (2013) A multidisciplinary framework to support the design of injection mold tools. Struct Multidiscip Optim 49(3):501–521
14. Martin JD, Simpson TW (2005) Use of Kriging models to approximate deterministic computer models. AIAA J 43(4):853–863
15. Lophaven SN, Nielsen HB, Sondergaard J (2002) DACE: a MATLAB Kriging toolbox, version 2.0. Informatics and Mathematical Modeling, Technical University of Denmark
16. Jones DR, Schonlau M, Welch WJ (1998) Efficient global optimization of expensive black-box functions. J Global Optim 13(4):455–492
17. Shi HZ, Xie SM, Wang XC (2013) A warpage optimization method for injection molding using artificial neural network with parametric sampling evalution strategy. Int J Adv Manuf Technol 65(1–4):343–353
18. AlKaabneh FA, Barghash M, Mishael I (2012) A combined analytical hierarchical process (AHP) and Taguchi experimental design (TED) for plastic injection molding process settings. Int J Adv Manuf Technol 66(5–8):679–694
19. Mathivanan D, Parthasarathy NS (2009) Prediction of sink depths using nonlinear modeling of injection molding variables. Int J Adv Manuf Technol 43(7–8):654–663
20. Guo W, Hua L, Mao HJ (2014) Minimization of sink mark depth in injection-molded thermoplastic through design of experiments and genetic algorithm. Int J Adv Manuf Technol 72(1–4):365–375

21. Deb K, Pratap A, Agarwal S, Meyarivan T (2002) A fast and elitist multiobjective genetic algorithm: NSGA- II. IEEE Trans Evol Comput 6(2):182–197

22. Fallah N, Honarparast S (2013) NSGA-II based multi-objective optimization in design of Pall friction dampers. J Constr Steel Res 89(10):75–85